Ab-Initio-Based Transferable Potential for Sodalites

Nick P. Blake,* Paul C. Weakliem, and Horia Metiu

Departments of Chemistry and Physics, University of California, Santa Barbara, California 93106

Received: August 13, 1997; In Final Form: September 12, 1997[⊗]

In this paper we derive a potential energy function for the frame atoms and the Na^+ ions in sodalite-type zeolites. We use Coulomb interactions between the charges on the frame atoms and the ions, a Buckingham potential for the pairwise interactions, and a three-body term that couples bending and stretching for the O−T−O unit (T = Si, Al). This potential ascribes realistic charges to the O atoms of the framework, with the charges on Si and Al fixed to ensure transferability of the potential to all possible Si/Al ratios. The remaining potential parameters are chosen to ensure (1) accurate fits to ab initio surfaces of model clusters calculated at the MP2-6-31G** level of theory, (2) accurate predictions as to NaCl-SOD, and (3) a reasonable infrared spectrum for NaCl-SOD and silica-SOD. We find that potentials that mimic bending with a purely angular dependent term give both poor fits to ab initio surfaces and vibrational frequencies in NaCl-SOD. Three-body potentials that include a coupling to bond lengths and pair potential schemes that include O−O interactions result in force fields that give both accurate fits to ab initio data, accurate structural predictions, and reasonable vibrational frequencies. The force field supplements the pairwise additive terms with a nearest neighbor O−T−O three-body potential that enforces the tetravalent sp^3 hybridization of the T atoms. The potential gives bond lengths that are accurate to within 0.01 Å, lattice constants to within 1%, vibrational frequencies that are within 3% of experiment, and bond angles that are accurate to within 1° of their X-ray-determined values.

I. Introduction

Zeolites have extensive industrial applications and interesting properties. To understand them, we need an adequate expression for the interaction energy between the frame atoms and the counterions. The large size of the unit cell and its low symmetry make ab initio calculations extremely time-consuming. Since modeling of transport properties of zeolites requires a huge number of force or energy evaluations, it is likely that in the near future most simulations will use semiempirical potential energy surfaces. These can be derived by fitting the measured properties of the solid, by fitting the potential energy surfaces calculated by ab initio methods, or both.

In the past 10 years there have been many attempts to determine realistic silicate and aluminosilicate force fields.[6−10,12,13,25,27−29,31,33,35,36,39,40,43,44] Some describe only the silicate framework[8,31,33,41,43,44] or, if applied to aluminosilicates, use an average T atom (where T = Si, Al).[9,10,28] The parameters defining these potentials have been provided by ab initio cluster calculations[27,33,43] or fitted to macroscopic data such as the structure,[27,34,35] the vibrational spectrum,[7,9] the elastic constants,[2] or the melting points.[44]

The functional forms used are fairly diverse. A harmonic or anharmonic potential is preferred[7−9,41] when spectroscopic data are fitted. Potentials that utilize structural data and/or ab initio data account for the partial ionicity of the aluminosilicates through a Coulombic potential[23,24,27,28,32,34,36,43,44] or else use derivative information to extract a generalized valence force field.[12,13,23,24] In addition, bonding is accounted for by using either a Buckingham[25,27] or a Lennard-Jones[28,35] form. Harmonic terms in the bending angles are sometimes used to represent the sp^3 hybridization of Si and Al atoms.[25,36]

Fits to the data provide a variety of values for the frame-atom charges used in the Coulomb energy. For the charge of the oxygen atoms, the following values have been proposed $-2.0e$ (ref 25), $-1.2e$ (refs 27, 43), $-0.8e$ (ref 44), $-0.6e$ (ref 32), and $-0.44e$ (refs 28, 34). This variation appears because the properties being fitted depend on the *sum* of all the terms in the potential energy. There is no guarantee that the parameters in each term in the sum have meaningful values, even when the sum fits the data well. In particular, a potential can have absurd charges on some of the atoms, and their ill effect is counteracted by unreasonable values for the parameters in other terms of the potential (e.g. the Buckingham interaction), leading to a sum that gives an adequate total energy. The proposed values for charges also differ because different methods are used to obtain them. Kramer et al. for example[27] treat the charges as an adjustable parameter in fitting the ab initio surface of $Si(OH)_4$, while No et al.[34] derive the charges from Huheey's electronegativity set by fixing the charge on Na and comparing with spectroscopic data.[34]

Ab initio cluster calculations can also provide inaccurate values for the Coulomb charges. The Mulliken populations—which are often used as charges in the Coulomb potential—can inaccurately represent the electrostatic fields around the clusters. In addition, finite clusters have substantially larger electronegativities than the infinite solids that they are designed to mimic.[26] With these considerations in mind it appears that partial charge schemes that set q_O between $-0.7e$ and $-0.9e$ are in agreement with high-level ab initio calculations or semiempirical electronegativity equalization techniques.[17] The quality of the charges on the frame atom can be tested by using them in calculations of the absorption spectrum of an electron solvated in various sodalites.[4,5,21,42] This quantity is particularly sensitive to the variation of the electrostatic field across the

[⊗] Abstract published in *Advance ACS Abstracts,* December 1, 1997.

S1089-5647(97)02681-3 CCC: $15.00
Published on Web 01/01/1998

zeolite cage, hence to the charges on the frame. The use of the oxygen charge in the range specified above leads to good agreement between the calculated spectrum and the measured one for dry sodalite and several halo-sodalites.[4,5,21,42] The other values do not.

Potential energy surfaces are obtained by adjusting the parameters in an empirical expression to fit either experimental data (we call these empirical potentials) or the energies obtained by ab initio calculations (we call these ab initio potentials), or sometimes both. The weaknesses and the advantages of these procedures are summarized below.

1. The number of parameters in the potential energy function often exceeds the number of truly independent experimental observables used in the fitting.[35,44] This is particularly true for tetraatomic systems such as the aluminosilicates. As a consequence, the empirical potentials for a diatomic system such as silica tend to work better than those for aluminosilicates. There is no limit to the amount of "data" that can be produced by ab initio calculations, other than the availability of computer power.

2. Empirical potentials obtained by fitting one type of crystalline structure often give poor results when applied to other structures. For example, the empirical potential derived by Catlow et al.[25] parametrized on silica fails to give a stable structure for NaX.[36] This happens because structure is a property depending on the total energy. The total energy can be adjusted to fit well a given structure, even though the bond and angle energy terms are in error; it is only the total energy that matters, and in fitting the structure, the errors in the individual terms are forced to cancel each other. However, there is no reason to expect that this cancellation will take place when the potential with parameters optimized for one structure is used to calculate the equilibrium structures of another compound. The ab initio potentials are obtained by fitting "data" in which specific, individual bond lengths or bond angles are varied; in principle, one can obtain correct parameters for the individual terms in the total energy. Such a potential is more likely to be transferable.

3. X-ray data, which is often used when designing an empirical potential, give a time-averaged structure which can differ from the true local structures; the mean configuration is usually not a minimum on the potential energy surface. Fitting the potential energy to such a mean structure will lead to erroneous parameters. This difficulty can be overcome by working only with structures having no ambiguities, such as those that have no structural disorder. But this is not always possible. For example, in the dehydrated sodalite there are fewer cations than cation binding sites, and the cation positions in the lattice are uncertain. In this case, fitting the average positions provided by the X-ray measurements invites trouble. Another example is silica sodalite which contains encapsulated ethylene glycol (EEC) within the sodalite cages. The presence of EEC is often ignored in potential parametrizations.[7,31] We do not know how ethylene glycol modifies the structure, but it is unlikely that these modifications are negligible; addition of water in dry sodalite, for example, causes a cage contraction of almost 0.3 Å. The ab initio potentials do not use X-ray data and are free of such pitfalls.

4. The parameters in the empirical potentials are obtained by fitting properties whose magnitude is affected only by very small displacements of the atoms around the equilibrium positions. The resulting potentials may not represent accurately processes in which large atomic displacements take place, i.e. cage-to-cage ion or neutral transport, bond breaking in the structure, melting, transition states, etc. There is no limit to how far a bond can be stretched or an atom displaced in the ab initio procedure.

5. The ab initio procedure has its own limitations that have no counterpart in the empirical one. The ab initio "data" are accurate only if the system has a small number of electrons. Because of this one is forced to work with small clusters. Often one suspects that these do not represent well the bulk material that one intends to simulate. The quality of the ab initio potential can be tested by calculating measurable properties, which have not been used in the fitting. Unfortunately, in many simulations one is interested in energies that are not available to direct measurement; testing that the potential works for measurable energies is necessary and success is reassuring, but it provides no guarantee that the potential works outside the range for which it has been tested.

In this paper we develop a set of potentials which we ultimately intend to use in a study of ion mobility in sodalitic zeolites. Such potentials must have reasonable values for the charges on the frame atoms since the electric fields they generate have an important influence on ion transport. It must describe well the ion−frame interactions for large ion displacements such as the passage of an ion from one cage to another, through the windows joining the cages. The window size and its deformation (the T−O−T and O−T−O (T = Si, Al) bending) when an ion passes through it must be modeled realistically. Finally the potential must describe well the energy associated with the cage contraction induced by ion solvation or the "swelling" caused by the temporary presence of an additional ion in the cage.

These requirements rule out the use of potentials determined exclusively by fitting experimental data, even though this method is adequate when used for other purposes. For this reason we have decided to derive potentials by fitting a functional form to "data" provided by ab initio Möller−Plesset second-order perturbation theory (MP2) calculations on small clusters. This provides "data" for large changes in the interatomic distances and gives reasonable values for the net charges of the atoms of the frame. Because the potential energy surfaces can be fitted using a variety of parameter sets, we supplement the fitting of the non-Coulombic interactions between distant atoms by comparing predictions with experimental data on the bulk material. The resulting potentials are tested by computing properties that have not been used for fitting and comparing them to experiment. In addition, the charges on the framework can be tested by calculating the absorption spectrum of electrons introduced by doping with alkali or through irradiation of the frame.[4,21]

There have been four attempts[12,13,23,24,27,43] at deriving ab initio potential energy surfaces for silicate and aluminosilicate systems. Unfortunately, while they provide good results for many observables, they do not fulfill the requirements we have specified for a potential that can be used to study ion transport.

Two of these potentials are obtained by fitting the energies calculated for $Si(OH)_4$, $Al(OH)_4^-$ (ref 27), or SiO_4^{2-} (ref 43). They fail to reproduce bulk parameters satisfactorily[2,6] unless supplemented by additional fitting to experimental data. It is interesting to note that both of these potentials are pairwise additive potentials. Potentials of this type fit the ab initio surfaces well and give satisfactory descriptions of many silica polymorphs, thus challenging the long held assertion that two-body central potentials cannot properly describe systems where directional bonding is present.[19] The best of the available potentials are based on HF SCF cluster calculations and experimental data.[27] In this work the bulk parameters (the charge and the O−O interaction) were adjusted to ensure that

both structural and elastic constants are faithfully reproduced for α-quartz. The remaining parameters are fitted to the ab initio potential-energy surface of small clusters. The potential set that is derived is impressive in both structural and dynamical predictions, especially for silica-based materials. Unfortunately, the charge on the oxygen atom is $q_O = -1.2e$,[27,43] which is almost twice as large as the charge that we consider reasonable. In addition the Na-SOD structure predicted by this potential is inaccurate. The inaccuracy of this potential can be traced back to both the charges used (these are not optimal for sodalite structures) and the fact that Al−O−Si bending is not considered in the fitting of the potential.

More recently, in a computational tour de force, Hill and Sauer[23,24] and Emoshin, Smirnov, and Bougard[12,13] have shown that a reliable, accurate, and transferable potential can be obtained without recourse to any experimental data through use of a generalized valence force field. The parameters in their silicate potential are fitted to give the equilibrium configuration, the equilibrium energy, and second derivatives of the energy with the coordinates, for nine clusters ranging from disilicic acid to a sodalite cage. The potential energy function includes three- and four-body terms and has 73 parameters for silica and 352 parameters for the aluminosilicates. Unfortunately neither of these potentials includes the interaction between the counterions and the frame, and the partial charges, when assigned to the framework atoms at all, are approximately half the Mulliken populations. For these reasons this potential cannot be used for the study of counterion transport.

In the subsequent sections we outline the derivation of a new force field that satisfies most of the above criteria by fitting ab initio data beyond equilibrium. We will show how this potential is able to accurately reproduce equilibrium properties such as structure and infrared spectra. The more extensive topic of ion transport is deferred to a forthcoming paper.

II. The Potential

II.1. The Functional Form of the Potential. The functional form chosen to describe the potential has consequences for both the additivity of the potential (i.e. two- vs three-body effects, etc.) and the length scales over which the various terms in the potential operate. Charge, for example, operates over the whole solid and hence many of the monomeric clusters, while the repulsion in typical Born−Mayer terms may only act on the nearest neighbors. We have found that a more long-range repulsion will ultimately favor larger lattice constants, while changing the attractive part of the potential from $-C/r^6$ to $-D/r^4$ will result in smaller lattice constants. These changes also have concomitant effects on the phonon spectrum for the solid.

The general functional form that we consider to best describe our system describes the interaction energy between two atoms i and j as

$$\Phi_{ij} = q_i q_j/r_{ij} + A_{ij}\exp(-r_{ij}/\rho_{ij}) - C_{ij}/r_{ij}^{\,6} + D_{ij}/r_{ij}^{\,5} + \sum_{n=1}^{N}\delta_{iO}\delta_{jO}\delta_{nT}\exp(-|r_{ij}|/\rho_{OO})\left[A_{ijn}\left(\cos(\theta_{ijn}) + \frac{1}{3}\right)^2\right] + \sum_{n=1}^{N}\delta_{iO}\delta_{nO}\delta_{jT}\exp(-|r_{in}|/\rho_{OO})\left[A_{ijn}\left(\cos(\theta_{ijn}) + \frac{1}{3}\right)^2\right] + \sum_{n=1}^{N}\delta_{jO}\delta_{nO}\delta_{iT}\exp(-|r_{jn}|/\rho_{OO})\left[A_{ijn}\left(\cos(\theta_{ijn}) + \frac{1}{3}\right)^2\right] \quad (1)$$

In eq 1 atomic units are assumed. The first term contains the long-range electrostatic interaction between the effective charges q_i and q_j separated by a distance r_{ij}. The second and third terms are the Buckingham potential representing bonding interactions as well as the interactions between nonbonded atoms. *(We have chosen r^{-6} and r^{-5} attractive terms over r^{-4} because the structures are more accurately reproduced.)* The last three terms depend on the angle between the O−T−O atoms and is active for nearest neighbor O and T atoms only. The delta function terms are there to ensure that only O−T−O combinations are considered; implicit in these terms is that i and j are not the same atom and that i,j,n represent the atom labels for *nearest neighbor atoms*. Its form is chosen simply because it fits the cluster points well, for *tetrahedrally coordinated Si* and Al atoms. The exponential r dependence in this expression ensures that the three-body term dies off at large O−O separations as well as mimicks the variation of the angular function for different bond lengths around the minimum. The three-body part extends only over the nearest neighbors of O−T−O type. In principle we also require a term to model the angular dependence of the Al−O−Si unit, since such bending is explicitly considered in the ab initio calculations. We have found that this is best mimicked when a Buckingham-type interaction for Al−Si is included. This is also computationally convenient since, in essence, we reduce the three-body interaction to a two-body interaction by noting the strong correlation of the bond angle and the Si−Al interatomic distance.

TABLE 1: Mean Calculated Charge Associated With the O in the $[(OH)_3-Si-O-Al-(OH)_3]^-$ Cluster as a Function of the Basis[a]

basis set	q_O/e
STO-3G (Mulliken)	−0.56
STO-3G (fit)	−0.79
6-31G** (Mulliken)	−0.72
6-31G** (fit)	−0.82

[a] The charges reported are the Mulliken populations. All calculations are performed at the MP2 level of theory. See the text for further information regarding the geometry considered.

II.2. Parameter Determination. We use a mixed ab initio−empirical method similar to that of Tsuneyuki et al.[43] and Kramer et al.[27] The energy dependence on the Si−O and Al−O bond lengths and the O−Si−O and O−Al−O angles is provided by MP2 cluster calculations, to avoid the errors introduced by the Hartree−Fock method used in earlier work.[27,43] Because the short-range interactions between the frame atoms are controlled by localized chemical bonds, it is possible to use the clusters $Si(OH)_4$, $Al(OH)_4^-$, $[(OH)_3Si-O-Al-(OH)_3]^-$, Na^+-$Si(OH)_4$, and Na^+Cl^- to determine the parameters in these interactions. The oxygen charge is obtained from ab initio calculations on the cluster $[(OH)_3Si-O-Al-(OH)_3]^-$. The outer oxygen atoms are "terminated" with hydrogen to simulate bonding to the rest of the frame; this has been shown to work quite well for these types of clusters.[1,37] *In general acceptable fits may be obtained with potential parameters that span quite different length scales; pinning down these length scales requires empirical input*, and these are determined by fitting experimental data on the bulk material.

The determination of the parameters in the potential (1) is done in several stages.

(a) The Charges on the Frame Atoms. The charge on O is fixed in accordance with the Mulliken population for the $[(OH)_3Si-O-Al-(OH)_3]^-$ cluster (see Table 1). Since extensive comparison with experiment indicates that the higher level calculations (such as MP2 or CI) using a large basis set give good values for dipole moments,[22] we use $-0.8e$ for the charge on O, in agreement with the values derived from the 6-31G**

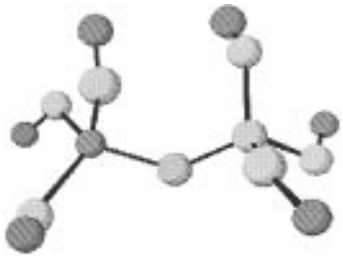

Figure 1. Ball and stick schematic of the geometry used for the ab initio calculations on $[(OH)_3Si-O-Al-(OH)_3]^-$.

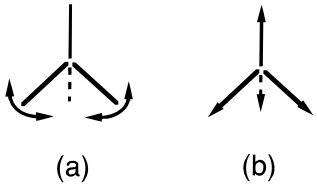

Figure 2. Illustration of (a) bending and (b) stretching modes of the $Si(OH)_4$ cluster considered in this paper.

HF-MP2 calculations. This oxygen charge is close to both that used in obtaining the correct absorption spectra for electrons introduced into the sodalite cages[3-5] and those obtained in Hartree−Fock calculations of the electronic structure of α-quartz.[11] The charge on silicon is fixed to ensure electroneutrality for the SiO_2 unit. Hence $q_{Si} = -2q_O$. The AlO_2 unit is taken to have a charge of −1, so that $q_{Al} = -2q_O - 1 = (q_{Si} - 1)$. Within this scheme all charges on the frame atoms are determined by the charge on the oxygen, and this charge scheme will ensure electroneutrality for all Si/Al ratios.

(b) The Counterion−frame Interactions. These are determined by fitting a function of the form (1) to the $Na^+\cdots Cl^-$ ab initio energy, for a range of interatomic separations from 1.5 to 10 Å. Similarly, the parameters in the $Na^+\cdots O$ interaction are determined by fitting (1) to the energies calculated for the $Na^+Si(OH)_4$ cluster, at configurations obtained by changing the $Na^+\cdots Si$ distance while keeping all other atomic positions fixed. The cluster used in this calculation contains hydrogen atoms, and their partial charges interact with the sodium ion. It is assumed that the Na^+-H and $Si-Na^+$ interactions are purely Coulombic and that all coulomb charges are accurately described using the Mulliken charges of the isolated cluster (the Na^+ ion charge fixed at $+1e$). The energy thus corrected is then used to fit the energy dependence on the Na^+-Si distance with the potential energy function given by eq 1.

(c) The O−O and O−T−O Interaction Parameters. Having determined the frame charges by the method described above, we no longer take them as variable parameters. Next we determine the parameters of the oxygen−oxygen interactions. To do this we use MP2 calculations of the energy of $Si(OH)_4$ or $Al(OH)_4^-$ as a function of the O−T−O angle, at constant O−H and *and three sets of T−O bond lengths.* The calculations were performed with the 6-311G** basis (after finding the optimum geometry). When we change the O−T−O angle, as indicated in Figure 2a, we also change the H−H distances. Because of the partial charges on the H atoms, there will be a Coulombic contribution to the change of the cluster energy. Since there is no hydrogen in the zeolite structure, we remove this effect of the hydrogen atoms by subtracting the Coulomb interactions due to the H atoms from the ab initio cluster energy. As with the Na^+-O interaction, all Coulomb interactions for the $Si(OH)_4$ or $Al(OH)_4^-$ clusters are assumed to be described using the *Mulliken* charges for these respective clusters. (This method of using Mulliken charges should be contrasted with the method used by van Beest et al.[27] where the charges in the cluster are assumed to be those of the bulk. The charge on H is therefore constrained to take the value $-q_O/2$, where q_O (the charge on O) is treated as a fitting parameter. In $Si(OH)_4$ the Mulliken charge is $0.235e$, while van Beest technique gives H a charge of $0.6e$.) The dependence of this corrected energy on the bond angle is shown in Figure 3. By fitting the corrected data with eq 1, we determine the parameters C_{OO}, ρ_{OO}, A_{OO}, and A_{OTO}. It happens that a good fit of the cluster data can be obtained for many pairs of values of the A_{OO} and ρ_{OO} parameters for the pair potential and A_{OTO} for the three-body potential. We will take advantage of this later to determine these parameters so that they will fit well the cluster data and also the some of the experimental bulk data. This fit to the bulk data is the last stage of the parameter determination, and we defer explaining it until later. Right now we proceed as if the optimization of the parameters in (1) to the cluster data has provided a unique set of values for all the parameters listed above.

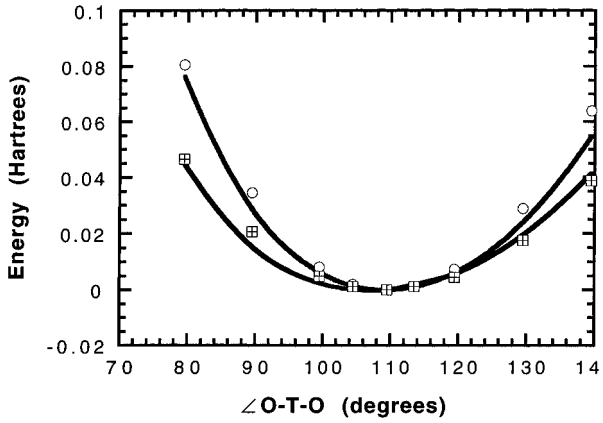

Figure 3. Energy for the scissor mode as a function of angle for the $Si(OH)_4$ cluster. The dots correspond to the ab initio calculations which are performed at the MP2/6-311G** level using GAUSSIAN 92;[16] the lines correspond to the analytical fits to these surfaces as defined by eq 1 in the text and the parameters defined in Table 2.

(d) The Parameters in the T−O Interaction. These are determined by fitting the results of ab initio calculations that determine the energy of $Si(OH)_4$ or $Al(OH)_4^-$ as a function of the Si−O (or Al−O) bond length. The bond length variation is performed symmetrically: all bonds in the tetrameric clusters are changed equally and in the same direction (see Figure 2b). This corresponds to an A breathing mode of the S_4 symmetry group. The optimum structure was obtained from an MP2/6-311G** calculation, which is known to give good geometry. The dependence of cluster energy on the bond length is shown in Figure 4. It is likely that these species are well described by the ab initio calculations; comparison with experiments is not possible because these molecules are too reactive.

(e) The Parameters in the Al−Si and Si−Si Interactions. These interactions were not sampled at an ab initio level since it is likely that the true bulk interaction is quite different from the interactions in clusters such as $[(OH)_3Si-O-Al(OH)_3]^-$. We therefore elected to treat these parameters empirically, adjusting them to give reasonable structures and infrared spectra. The Al−Si interaction and the Si−Si interaction were taken to be of Buckingham form. As with the earlier work of Nicholas et al., we found that this interaction is important in setting the gap between the symmetric and asymmetric modes in the solids.[31] Since the O−O interactions also extend over next nearest neighbors, the T−T′ parameters needed adjusting every

TABLE 2: Pairwise Additive Parameters and the Three-Body Parameters in the Potential Energy Function Eq 1 (Atomic Units Are Used Throughout)

(a) Pairwise Additive Parameters[a]

$i-j$	A_{ij} (Hartrees)	ρ_{ij} (bohr)	C_{ij} (Hartrees bohr^6)	D_{ij} (Hartrees bohr^5)	q_i (e)
Si−Al	31.776	0.775 000	0.000	14.086 11	
O−O	100.217	0.600 000	200.000	0	$q_O = -0.8$
Si−O	1009.663	0.362 294	243.572	0	$q_{Si} = +1.6$
Al−O	1052.596	0.391 099	427.403	0	$q_{Al} = +0.6$
Na−O	102.280	0.505 060	66.603	0	$q_{Na} = +1.0$
Cl−Na	120.420	0.591 590	301.710	0	$q_{Cl} = -1.0$
Si−Si	1029.000	0.761 020	24 102.000	0	

(b) Three-Body Parameters

A_{OSiO} (Hartrees)	A_{OAlO} (Hartrees)
−62.315	−89.094

[a] The range of validity for these parameters is for the bulk parameters (Si−Si, O−O, and Si−Al) is $r < 7$ bohr; Si−O $2.5 < r < 3.7$ bohr, Al−O $2.5 < r < 4.0$ bohr, Na−O $r > 3$ bohr, NaCl $r > 3$ bohr. For the three-body interactions $80° < \theta < 140°$.

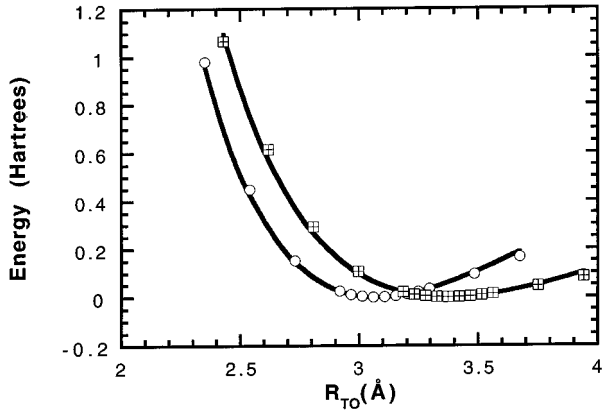

Figure 4. Energy as a function of the T−O bond length for stretching in the A_1 mode (see Figure 2) for the $Si(OH)_4$ and $Al(OH)_4^-$ clusters. The diamonds denote the ab initio configuration energies for the $Si(OH)_4$ cluster, and the dots, the corresponding ab initio energies for the $Al(OH)_4^-$ cluster. All calculations are performed at the MP2/6-311G** level using GAUSSIAN 92.[16] The lines correspond to the analytical fits to these surfaces as defined by eq 1 in the text and the parameters defined in Table 2.

time the O−O interaction parameters were modified. As a consequence of this deficit in our procedure, the fitting is done iteratively. Thus ρ_{OO} is an independent variable, and we choose a reasonable value for ρ_{OO} and fit the remaining O−O parameters to the ab initio points. The remaining T−O cluster parameters are fitted to the stretching modes as described above, and then finally the potential parameters defining the T−T′ interaction are adjusted to bring predictions in best accord with the bulk properties of the NaCl-SOD and silica-SOD. This gives a certain "goodness of fit". Then we change ρ_{OO} and repeat the procedure. This goes on until we obtain the best fit for the cluster properties and the bulk properties.

The detailed implementation of this scheme is explained below. Since we have already discussed how the fits to the ab initio results are made, we just concentrate on the fitting to the bulk properties. For this we use the cost function

$$\chi = w_{\text{freq}}\sum_{i=1}^{N}|\omega_i^{\text{exp}} - \omega_i^{\text{theory}}|^2 + w_{\text{force}}\sum_{i=x,y,z}\sum_{j=1}^{46}|F_{ij}|^2 + w_{\text{lattice}}|L_{\text{exp}} - L_{\text{theory}}|^2 \quad (2)$$

This depends on the bulk parameters (all others are held fixed) and measures how well the calculated values agree with the measured ones, for a given set of parameter values. Here ω_i^{exp} is the frequency of the ith infrared active mode in NaCl-SOD, and ω_i^{theory} is the predicted frequency for this mode. F_{ij} is the ith Cartesian component of the total force on the atom j of the unit cell, and L_{exp} and L_{theory} are the experimental and predicted lattice constants for the NaCl-SOD and Na-SOD. w_{freq}, w_{force}, and w_{lattice} are weighting coefficients used to emphasize or deemphasize the relative importance of the various contributions to the cost function. We picked them to make all terms equally important. This cost function is minimized with respect to the bulk parameters by using a simplex algorithm.

We outline now briefly how the quantities present in the cost function are calculated. The lattice constants were obtained by means of five fixed-volume energy minimizations with box lengths of $L + n\delta$, where $n = (0, 1, 2)$, $\delta = 0.005\Lambda$, and $L =$ 8.88 Å (NaCl-SOD) or 9.122 Å (Na-SOD). All energy minimizations were performed using a steepest descent algorithm implemented for the unit cell. The harmonic frequencies needed when fitting the IR spectra are the eigenvalues of the dynamic matrix (evaluated at the $\Gamma(\mathbf{q}=\mathbf{0})$ point):[30]

$$D_{ij}(\mathbf{q},k,k') = (m(k)\, m(k'))^{-1/2}\sum_{l}\frac{\partial^2\Phi}{\partial u_j(0,k)\,\partial u_i(l,k')}\exp(i\mathbf{q}\cdot\mathbf{A}(l)) \quad (3)$$

where $u_j(lk')$ is the displacement vector for Cartesian coordinate j $(=x,y,z)$ of the atom k' of mass $m(k')$, in the unit cell labeled l, and whose coordinates are $A(l)$ relative to some arbitrary origin. Φ is the potential energy of the crystal. The second derivatives are evaluated at the equilibrium configuration. The Coulomb interactions in the dynamic matrix are evaluated by using the Ewald method.

III. The Force Field

In what follows we look at some of the structural and dynamic predictions for the sodalitic systems silica-sodalite, NaCl-SOD, Na-SOD, and silica-SOD. The parameters for both the pairwise and three-body parts of the potential are presented in Table 2a,b, respectively. The fits to the potential energy surfaces of the clusters are shown in Figures 3 and 4. As we have already emphasized, the *sum* of various terms is used to fit the data, and the parameters in each term are physically correct only if the functional forms used in the sum have the correct form. As the correct form is not known, one should regard with skepticism a physical interpretation of the parameters coming out of these

TABLE 3: Selected Atomic Bond Lengths (Å), Framework Bond Angles (deg), and the Bulk Modulus for NaCl-SOD[a]

NaCl-SOD	expt	BMW	LDA	KFvB
lattice constant (Å)	8.88	8.88	8.92	8.77
bulk modulus (Mbar)	0.55	0.66		0.82
Si−O (Å)	1.62	1.61	1.59	1.57
Al−O (Å)	1.74	1.74	1.78	1.76
∠O−Si−O	2 × 113.0	2 × 112.13	2 × 114.6	2 × 111.6
	4 × 107.7	4 × 108.24	4 × 107.0	4 × 108.4
∠O−Al−O	2 × 111.0	2 × 110.16	2 × 111.3	2 × 109.5
	4 × 108.7	4 × 109.0	4 × 108.6	4 × 109.4
∠Si−O−Al	138.2	138.9	134.6	136.1

[a] Experimental values are taken from Hassan and Grundy,[20] the results of density functional calculations (in the linear density approximation (LDA)) are from Filippone et al.,[15] KFvB refers to the predictions made using the aluminosilicate potentials of Kramer et al.,[27] and BMW are the predictions made with our potential.

TABLE 4: Comparison of the Experimental Positional Parameters for O and Na^+ for NaCl-SOD with Those Predicted Using the Current Potential[a]

positional parameter	expt	BMW
(a) oxygen (24h)		
	0.1390	0.1380
	0.4383	0.4398
	0.1494	0.1488
(b) sodium (8e)		
	0.1778	0.1749
	0.1778	0.1749
	0.1778	0.1749

[a] The space group is $P\bar{4}3n$. Symmetry labels are given in parentheses.

fits. Nonetheless one result is worth noting; namely if a three-body bending term is used, then it is necessary to use a functional form that couples bond lengths and bond angles. Potentials that include an angular dependent term with no bond length dependence give poor fits to the ab initio surfaces and very poor descriptions of the vibrational frequencies in sodalite materials and are not considered further.

The final functional form of the resulting potential is similar to that obtained by Tsuneyuki et al. and Kramer et al.[27,43] However, the charges on the frame atoms are different, and this of course causes a change in the values of all parameters. To find out how good the potential is, we compare its structural predictions with those of other calculations and with experimental results. Comparison with the data for the dry sodalite Na-SOD is less significant than that for NaCl-SOD and silica-SOD. This is because in Na-SOD three Na ions can occupy four equivalent sites in the cage, and in interpreting the results of the X-ray measurements one must make assumptions about the positions of the counterions. This introduces uncertainties in the structures provided by the measurements.

(a) NaCl-SOD. The results for NaCl-SOD for selected bond lengths and angles are presented in Table 3, while the calculated and experimental cell parameters for O and Na^+ a given in Table 4. Direct comparison of the experimental XRD[20] with the structural predictions made by us, Filippone et al.,[15] and Kramer et al.[27] reveals that the agreement with experiment is good and our potential does slightly better than the other calculations. We are rather pleased to see this, since we believe that the charges used in our potential are more accurate than those used by Kramer et al., while the MP2 6-311G** calculations on which the potential is based are typically more accurate than LDA-type calculations. As is typical with ab initio-type calculations, the bond lengths are slightly underestimated with this potential (typically 0.01 Å). This is the type of accuracy to be expected from the current level of ab initio calculation. The calculated bulk modulus is also much closer to experiment than that predicted by the potential of Kramer et al. This is in accord with the observation that more realistic partial charges give rise to more realistic elastic constants.[19]

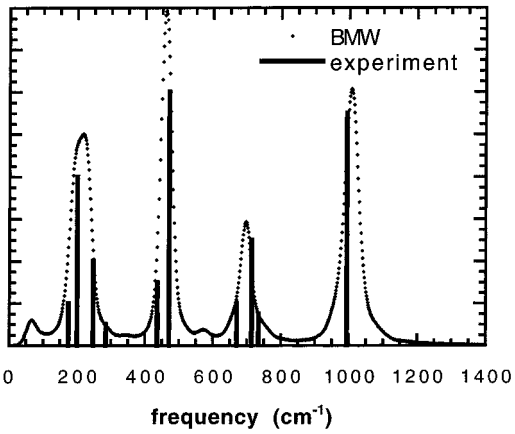

Figure 5. Computed IR vibrational spectrum for NaCl-SOD. The vertical lines indicate the peak positions in the IR spectrum and do not relate to the experimental intensities.[18] See the text for the computational details.

TABLE 5: Comparison of the Predicted Bond Lengths and Tilt Angles for Silica Sodalite Using the Current Potential (Denoted BMW) with the XRD Data of Richardson et al.[38] [a]

SOD	expt	BMW	HS	KFvB
lattice constant (Å)	8.83	8.91	9.06	8.99
Si−O (Å)	1.59	1.60	1.620	1.612
∠Si−O−Si (deg)	159.7	161.0	162.0	163.1

[a] HS refers to the results of the structural minimizations made using the Hill and Sauer potential,[23] and KFvB are those for potential derived by Kramer et al.[27]

In Figure 5 we show the computed IR vibrational spectrum for NaCl-SOD along with the experimental peak positions.[18] This we have calculated these from a molecular dynamics calculation, by taking a Fourier transform of the dipole−dipole autocorrelation function. Because of the short simulation time there is insufficient resolution to resolve the δ(O−T−O) double peak and the three ν_S(T−O) modes. Since this is a classical calculation, the intensity of the peaks in the absorption cross section need not agree with the experiment; however, the peak frequencies should, if the potential is accurate. All of the framework and intracavity ion frequencies are faithfully reproduced with this potential. The calculated values are within 15 reciprocal centimeters from the measured ones. These inaccuracies are close to those expected in ab initio calculations.

(b) Silica-SOD. In Table 5 we compare the structure that minimizes our potential with the experimental data obtained by Richardson et al.[38] for the silica sodalite and with calculations using the potentials derived by Kramer et al.[27] and by Hill and Sauer.[23] Again, the agreement with experiment is good, and our results are slightly closer to the experiment than those provided by the other calculations. Unfortunately this success is not as significant as one would like. The compound used in the experiments had ethylene glycol incorporated in the cages and the calculations do not. We can say that the experiment and the calculations agree only if the presence of the ethylene glycol does not affect cage size. In Figure 6 we show the computed IR vibrational spectrum for silica-SOD along with the experimental peak positions.[31] The present potential is seen

TABLE 6: Comparison of the Experimental Positional Parameters for O and Na^+ for Na-SOD at 614 K[14] with Those Predicted Using the Current Potential[a]

positional parameters	experiment	BMW (symmetric 450 K)	BMW (asymmetric 500 K)	vB (symmetric 450 K)
O (24h)				
x	0.1450	0.1437 ± 0.0015	0.1441 ± 0.0017	0.1355 ± 0.0019
y	0.4890	0.4913 ± 0.0061	0.4842 ± 0.0108	0.4344 ± 0.0029
z	0.1550	0.1558 ± 0.0015	0.1543 ± 0.0017	0.1474 ± 0.0016
Na (8e)				
x	0.225	0.2277 ± 0.0079	0.2250 ± 0.010	0.2210 ± 0.011
y	0.225	0.2277 ± 0.0079	0.2250 ± 0.009	0.2250 ± 0.008
z	0.225	0.2277 ± 0.0079	0.2250 ± 0.010	0.2210 ± 0.011

[a] The predicted parameters represent dynamic averages from MD trajectories along with their standard deviations. The space group is $P\bar{4}3n$. Symmetry labels are given in parentheses. The terms symmetric and asymmetric refer to the two types of ion ordering possible in the unit cell.

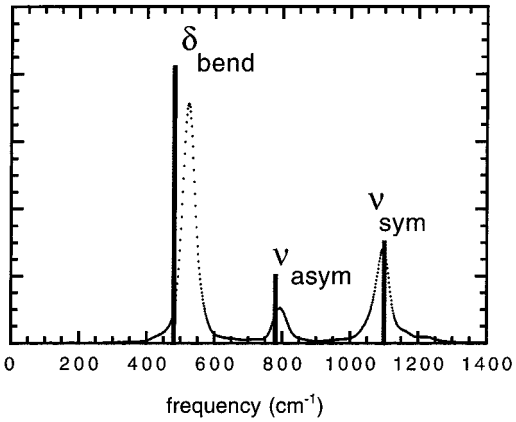

Figure 6. Computed IR vibrational spectrum for silica-SOD. The vertical lines indicate the peak positions in the IR spectrum and do not relate to the experimental intensities.[31] See the text for the computational details.

to give a reasonable representations of symmetric and asymmetric stretching frequencies, while the bending mode is predicted to be 20 cm^{-1} higher than observed.

(c) Na-SOD. The comparison of the calculations with the results derived from experiment is more difficult for the dry sodalite. Uncertainties are caused by the fact that three counterions in each cage have four sites to bind to. One can describe the structure of the system by indicating which site is vacant in each cage. Several possibilities then exist. The vacancies may be ordered, meaning that their position is periodic in space. The ordered structures may be organized in domains. There may be static disorder, i.e. the empty sites are not on a periodic lattice. And there may be dynamic disorder: the vacant site moves around in the cage on the time scale on which the data are taken. Such motions could be independent or correlated. There is more, but we hope that this list gives a fair idea of the difficulties an experimentalist faces in deriving a structure from the experimental data. The existing structure[14] was obtained by assuming that, during the time the X-ray data were taken, the vacancy migrates and occupies each of the four sites with equal probability. While such an assumption is reasonable as a first pass at extracting structural information from the X-ray diffraction data, it does not give results that can be used to determine how good a potential is in reproducing the results in *detail*. Mindful of these pitfalls we nevertheless present a comparison of our calculations with the experimental results.

We have found that the dry sodalite has the lowest energy when the vacant sites are ordered. This we have found to be true even up to supercells of 3 × 3 × 3 unit cells. All subsequent calculations are restricted to these ordered structures. Analysis of the Hessian matrix for the minimized structure obtained by constraining the unit cell to be cubic leads to a number of imaginary frequencies. This indicates that *P*43*n* is not the preferred structure for dry sodalite, according to this potential. This is in accord with recent X-ray experiments which show a phase change below 600 K (the temperature used in the Felsche work[14]).

TABLE 7: Comparison of the Predicted Bond Lengths and Bond Angles for the Na-SOD with the XRD Data of Felsche, Luger, and Baerlocher[14] [a]

Na-SOD	expt	BMW	KFvB	LDA
lattice constant(Å)	9.12	9.12	8.76	9.30
⟨Si−O⟩ (Å)	1.58	1.61	1.61	1.59
⟨Al−O⟩ (Å)	1.71	1.73	1.74	1.78
⟨∠Si−O−Al⟩	156.3	149.4	135.5	154.2

[a] The LDA results are taken from Filippone et al.[15] KFvB refers to the predictions made using the aluminosilicate potentials of Kramer et al.,[27] and BMW are the predictions made with our potential.

The structural disorder results in a large variation in the Si−O−Al angles, depending on whether there is a Na^+ cation in proximity to that O atom. This leads to a distribution of fractional coordinates for O in the true cell. Since it is the structural parameters that are extracted from XRD, it is these that should be compared and not so much actual bond lengths and bond angles. The structural averaging is therefore accomplished through evaluation of the *average* positional parameters for the *P*43*n* space group. The dynamical averaging is accounted for (in part at least) through dynamic averages of molecular dynamics NVE trajectories at 600 K.

In Table 6 we compare the average positional parameters, while in Table 7 the arithmetic means of the bond lengths and angles are presented. The current potential implies a large variance associated with one of the fractional coordinates for O; this can be associated with a facile bending of the Si−O−Al bond and a large variance in the Na positional parameters. The predicted and observed positional parameters are in reasonable accord. The potential predicts the lattice constant to within 0.5%, and the positional parameters agree to within a standard deviation. The potential of Kramer et al. however does not do well for this material. It makes an error of 4% in the lattice constant. A consequence of this is that the positional parameters for O agree poorly with experiment. The present potential implies that the predicted bond lengths will be close to those calculated for NaCl-SOD and that the apparent deviation from experiment is more a consequence of the deviation of the true structure from the $P\bar{4}3n$ space group symmetry. This assertion should be easily verifiable by examining the chemical shift associated with the Al and Si nuclei in this material.

In Figure 7 we present the calculated IR spectrum for dry sodalite along with the peak positions as measured by Fillipone et al.[15] As with NaCl-SOD the computed spectrum is in better agreement with experiment than recent density functional calculations.[15]

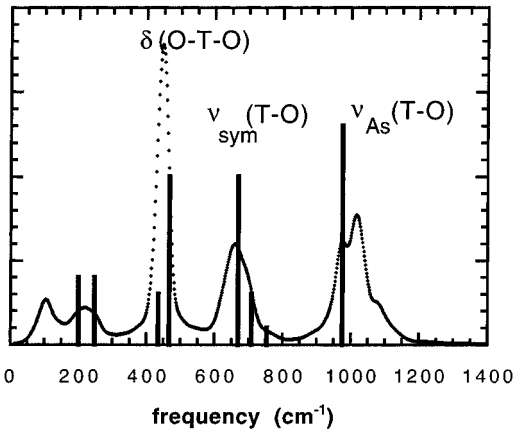

Figure 7. Computed IR vibrational spectrum for Na-SOD. The vertical lines indicate the peak positions in the IR spectrum and do not relate to the experimental intensities.[15] See the text for the computational details.

IV. Conclusions

Our intention in this paper has been to produce a potential energy function for sodalites that can be used to simulate the motion of the counterions. To be successful such a potential must use accurate charges for the frame atoms, give good energy values for large changes in the positions of the counterions, and represent well the change in cage and window sizes as an ion moves from one cage to another. To accomplish this task, we fitted the parameters of a simple functional form to energies obtained from high-level ab initio calculations on small clusters and to certain experimental observables. The use of the ab initio results allowed us to obtain reliable charges for the frame atom and good bonding energies and distances. The charges obtained in this way lead to correct spectra for electrons solvated in sodalites.[4] The parameters describing energy changes with the bond angles were obtained by fitting both the ab initio data and some experimental results. To test the quality of the potential, we calculated the structures of several sodalites and the vibrational spectrum for NaCl-SOD, silica-SOD, and Na-SOD and compared the results to experiment. The agreement is very good. Our results are *slightly* better than the ones provided by the best existing potentials or the density functional calculations. Thus, the improved frame charges and the ability to deal with large displacements in the frame atom and ion position did not impair the ability of the potential to make both good structural and dynamical predictions.

This potential is currently being applied to the topic of ion mobility in aluminosilicates and will be discussed in a forthcoming paper. Beyond this it is our hope that the current force field can be used to model aluminosilicate systems that are beyond the reach of current ab initio technology, with an accuracy comparable to first-principles techniques. Indeed research on the performance of this potential in faujasite structures is currently under way.

Acknowledgment. This research was supported in part by the Office of Naval Research and by the National Science Foundation.

References and Notes

(1) Alvarado-Swaisgood, A. E.; Barr, M. K.; Hay, P. J.; Redondo, A. *J. Phys. Chem.* **1991**, *95*, 10031−10036.

(2) Beest, B. W. H. v.; Kramer, G. J.; Santen, R. A. v. *Phys. Rev. Lett.* **1990**, *64*, 1955.

(3) Blake, N. P.; Metiu, H. *J. Chem. Phys.* **1994**, *101*, 223.

(4) Blake, N. P.; Srdanov, V. I.; Stucky, G. D.; Metiu, H. *J. Phys. Chem.* **1995**, *99*, 2127.

(5) Blake, N. P.; Srdanov, V. I.; Stucky, G. D.; Metiu, H. *J. Chem. Phys.* **1996**, *104*, 8721−8729.

(6) Chelikowsky, J. R.; King, H. E.; Glinnemann, J. *Phys. Rev. B* **1990**, *41*, 10866−10869.

(7) Creighton, J. A.; Deckman, H. W.; Newsam, J. M. *J. Phys. Chem.* **1994**, *98*, 448−459.

(8) de Man, A.; van Santen, R. A. *Zeolite* **1992**, *12*, 269.

(9) Demontis, P.; Suffritti, G. B.; Quartieri, S.; Fois, E. S.; Gamba, A. *Zeolites* **1987**, *7*, 522−527.

(10) Demontis, P.; Suffritti, G. B.; Quartieri, S.; Fois, E. S.; Gamba, A. *J. Phys. Chem.* **1988**, *92*, 867−871.

(11) Dovesi, R.; Pisani, C.; Roetti, C.; Silvi, B. *J. Chem. Phys.* **1987**, *86*, 6967.

(12) Ermoshin, A.; Smirnov, K. S.; Bougard, D. *Chem. Phys.* **1996**, *209*, 41−51.

(13) Ermoshin, V. A.; Smirnov, K. S.; Bougard, D. *Chem. Phys.* **1996**, *202*, 53−61.

(14) Felsche, J.; Luger, S.; Baerlocher, C. *Zeolites* **1986**, *6*, 367.

(15) Fillopone, F.; Buda, F.; Iarlori, S.; Moretti, G.; Porta, P. *J. Phys. Chem.* **1995**, *99*, 12883−12891.

(16) Frisch, M. J.; Trucks, G. W.; Head-Gordon, M.; Gill, P. M. W.; Wong, M. W.; Foresman, J. B.; Johnson, B. G.; Schlegel, H. B.; Robb, M. A.; Replogle, E. S.; Gomperts, R.; Andres, J. L.; Raghavachari, K.; Binkley, J. S.; Gonzalez, C.; Martin, R. L.; Fox, D. J.; Defrees, D. J.; Baker, J.; Stewart, J. J. P.; Pople, J. A. *Gaussian 92*; Gaussian, Inc.: Pittsburgh, PA, 1995.

(17) Genechten, K. v.; Mortier, W. J.; Geerlings, P. *J. Chem. Phys.* **1987**, *86*, 5063.

(18) Godber, J.; Ozin, G. A. *J. Phys. Chem.* **1988**, *92*, 2841−2849.

(19) Guido, R.; Valle, D.; Andersen, H. C. *J. Chem. Phys.* **1991**, *94*, 5056−5059.

(20) Hassan, I.; Grundy, H. D. *Acta Crystallogr.* **1984**, *B40*, 6−13.

(21) Haug, K.; Srdanov, V. I.; Stucky, G. D.; Metiu, H. *J. Chem. Phys.* **1992**, *96*, 3495−3501.

(22) Hehre, W. J.; Radom, L.; Schleyer, P. v. R.; Pople, J. A. *Ab Initio Molecular Orbital Theory;* John Wiley & Sons: New York, 1986.

(23) Hill, J. R.; Sauer, J. *J. Phys. Chem.* **1994**, *98*, 1238−1244.

(24) Hill, J. R.; Sauer, J. *J. Phys. Chem.* **1995**, *99*, 9536−9550.

(25) Jackson, R. A.; Catlow, C. R. A. *Mol. Sim.* **1988**, *1*, 207−276.

(26) Janssens, G. O. A.; Baekelandt, B. G.; Toufar, H.; Mortier, W. J.; Schoonheydtr, R. A. *J. Phys. Chem.* **1995**, *99*, 3251−3258.

(27) Kramer, G. J.; Farragher, N. P.; Beest, B. H. W. v.; Santen, R. A. v. *Phys. Rev. B* **1991**, *43*, 5068−5080.

(28) Lee, S. H.; Moon, G. K.; Choi, S. G.; Kim, H. S. *J. Phys. Chem.* **1994**, *98*, 1561−1569.

(29) Mabilia, M.; Pearlstein, R. A.; Hopfinger, A. J. *J. Am. Chem. Soc.* **1987**, *109*, 7690.

(30) Maradudin, A. A.; Montroll, E. W.; Weiss, G. H.; Ipatova, I. P. *Theory of Lattice Dynamics in the Harmonic Approximation*; Academic Press: New York, 1971.

(31) Nicholas, J. B.; Hopfinger, A. J.; Trouw, F. R.; Iton, L. E. *J. Am. Chem. Soc.* **1991**, *113*, 4792−4800.

(32) Nicholas, J. B.; Trouw, F. R.; Mertz, J. E.; Iton, L. E.; Hopfinger, A. J. *J. Phys. Chem.* **1993**, *97*, 4149−4163.

(33) Nicholas, J. B.; Winans, R. E.; Harrison, R. J.; Iton, L. E.; Curtiss, L. A.; Hopfinger, A. J. *J. Phys. Chem.* **1992**, *96*, 7958−7965.

(34) No, K. T.; Huh, Y. Y.; Jhon, M. S. *J. Phys. Chem.* **1989**, *93*, 6413−6417.

(35) No, K. T.; Kim, J. S.; Huh, Y. Y.; Kim, W. K.; Jhon, M. S. *J. Phys. Chem.* **1987**, *91*, 740.

(36) Ooms, G.; Santen, R. A. v.; Ouden, C. J. J. d.; Jackson, R. A.; Catlow, C. R. A. *J. Phys. Chem.* **1988**, *92*, 4462−4465.

(37) Redondo, A.; Hay, P. J. *J. Phys. Chem.* **1993**, *97*, 11754−11761.

(38) Richardson, J. W.; Pluth, J. J.; Smith, J. V.; Dytrych, W. J.; Bibby, D. M. *J. Phys. Chem.* **1988**, *92*, 243−247.

(39) Sauer, J. *Chem. Phys. Lett.* **1983**, *97*, 275.

(40) Sauer, J. *Chem. Rev.* **1989**, *89*, 199−255.

(41) Smirnov, K. S.; Bougeard, D. *J. Phys. Chem.* **1993**, *97*, 9434−9440.

(42) Srdanov, V. I.; Haug, K.; Metiu, H.; Stucky, G. D. *J. Phys. Chem.* **1992**, *96*, 9039.

(43) Tsuneyuki, S.; Tsukada, M.; Aoki, H.; Matsui, Y. *Phys. Rev. Lett.* **1988**, *61*, 869.

(44) Vashista, P.; Kalia, R. K.; Rino, J. P.; Ebbsjö, I. *Phys. Rev. B* **1990**, *41*, 12197−12209.